



Alexandria University
Alexandria Engineering Journal

www.elsevier.com/locate/aej
www.sciencedirect.com



CFD-Study of the H-Rotor Darrius wind turbine performance in Drag-Lift and lift Regime: Impact of Type, thickness and chord length of blades

Pedram Ghiasi^{a,*}, Gholamhassan Najafi^a, Barat Ghobadian^a, Ali Jafari^b,
 Rizalman Mamat^{c,d}, Mohd Fairusham Ghazali^d

^a Department of Biosystems Engineering, Tarbiat Modares University, Tehran P.O. Box 111-14115, Iran

^b Department of Agricultural Engineering, University of Tehran, Karaj P.O. Box 6619-14155, Iran

^c School of Mechanical Engineering, Ningxia University, China

^d Centre for Research in Advanced Fluid and Process, University Malaysia Pahang, Lebuhraya Tun Razak, Gambang, Kuantan 26300, Pahang, Malaysia

Received 14 June 2022; revised 7 September 2022; accepted 2 October 2022

Available online 28 October 2022

KEYWORDS

Renewable Energy;
 Clean energy;
 Vertical axis wind turbine

Abstract The high power coefficient of the Darrius vertical axis wind turbine lift regime has prompted researchers to concentrate their efforts on this regime, despite the fact that these turbines suffer from major problems in the drag-lift regime. In the present study, in addition to exploring the performance of the Darrius type wind turbine at blade tip speeds Ratio above 1, the effect of design factors on its performance at TSRs below 1 is also investigated. The results were extracted from numerical analysis recruiting Fluent software and the k-w SST turbulence model. The effect of blade type, thickness, and chord length on turbine performance has been investigated. The blade angle of attack (AOA) at TSR less than one was calculated using a new equation, and the results were evaluated. The numerical study of the Darrius wind turbine showed that increasing the chord length for symmetric and asymmetric airfoils from 0.1 to 0.2 m enhances the turbine performance in drag-lift regime, whereas decreasing chord length improves turbine performance at higher TSRs. The blade with a curvature of 4 % and a chord length of 0.1 m has the best performance at TSR 2.25. Increasing the thickness from 18 to 22 % of chord length exerts a negative influence on the turbine's performance in both regimes, and at lower TSRs, NACA0018 airfoil with a chord length of 0.2 m was of the optimum performance in the drag-lift regime.

© 2022 THE AUTHORS. Published by Elsevier BV on behalf of Faculty of Engineering, Alexandria University. This is an open access article under the CC BY license (<http://creativecommons.org/licenses/by/4.0/>).

* Corresponding author.

E-mail address: p.ghiasi@modares.ac.ir (P. Ghiasi).

Peer review under responsibility of Faculty of Engineering, Alexandria University.

<https://doi.org/10.1016/j.aej.2022.10.013>

1110-0168 © 2022 THE AUTHORS. Published by Elsevier BV on behalf of Faculty of Engineering, Alexandria University.

This is an open access article under the CC BY license (<http://creativecommons.org/licenses/by/4.0/>).

1. Introduction

Reducing reliance on the use of fossil fuels can be the result of employing more wind energy [1]. Wind energy extraction is a

critical concern nowadays, and wind turbines are among primary tools in this respect [2]. Large-scale wind power generation is generally conducted recruiting horizontal axis wind turbines, while vertical axis wind turbines provide more flexibility and are employed for a variety of purposes [3–4]. The rotation of vertical axis wind turbines occurs within two regimes of drag and lift [5–6]. In general, the blade tip speed of vertical axis wind turbines in drag regime (such as Savonius) does not exceed 1 and they can rotate at low wind speeds [7–8]. The functioning of a Darrius type wind turbine with straight blades (H-Rotor) is within the drag and lift regimes, and therefore, the analysis of aerodynamic forces on the blades is particularly of difficulty [9]. When Darrius wind turbines are categorized according on their rotational operating force, two modes with respect to blade tip speed (TSR) below 1 and TSR above 1 are established. When TSR is less than one, lift force and drag force operate simultaneously, whereas when TSR is more than one, lift force is the sole source of turbine rotation. The Darrius wind turbine with a straight blade operates properly when the blade tip speed exceeds 1 and enters the lift regime [10]. Before the blade tip speed reaches 1, only half of the travel path can be covered by the rotor due to the lift force (the blades move in the opposite direction of the wind), while the other half is supported by the drag force [11]. However, once the blade tip speed of 1 is reached, the lift force operates the entire rotation path. The primary issues with Darrius type vertical axis wind turbines are self-rotation and inability to achieve the starting torque for rotation at high speeds, which is caused by incorrect turbine operation at TSRs less than 1. To address the existing issue, numerous studies have been carried out, each of which investigated the effect of one of the design parameters on these modes. In some, the influence of rotor solidity [12], airfoil shape [13–14], and rotor dimensions ratio [15] on the self-rotation parameters and performance of this type of turbine have been explored, and an acceptable interval was then proposed with the aim of solving this problem. Another proposed solution to eliminate self-rotation issues and increase the Darrius wind turbine performance is a variable pitch angle, which has been the focus of research by designers and specialists in this field [16–18]. Despite this, proper analysis of Darrius type wind turbines at TSRs below 1 can still suggest innovative approaches to overcome the problems of this type of turbines.

Rotor solidity is affected by various factors such as chord length, number of blades and rotor diameter. Increasing the chord length in turbines with two and three blades improves the performance to some extent, however, the wind turbine performance will decline with increasing chord length [19]. Wind turbines with more blades have better performance at low TSRs, but the performance of turbines with additional blades decreases at high TSRs [20,21]. Enhanced turbine size ratio increases power coefficient at TSRs less than 2, but not at TSRs more than 2. This result was obtained from panel method analysis on Darrius turbines [22]. In general, wind turbine performance improves at high TSRs by reducing rotor solidity [19–21,23–26]. Furthermore, while high-solidity rotors can achieve a stable rotary speed faster, they perform worse at lower blade tip speeds [27]. The self-rotation parameter can be altered by employing different airfoils. Of the three NACA symmetric and asymmetric airfoils, the EN0005 takes the least amount of time to achieve a stable rotary speed. However, taking into account other parameters such as power coefficient

and stability in torque production, the Airfoil S-1046 provides the best performance for the wind turbine. This is the result of numerical research on a Darrius wind turbine with a straight blade [28]. Others [13–29–30] support the finding that the probability of rotation at low Reynolds for curved airfoils is higher than for symmetrical airfoils. Because of the greater angle of attack, dynamic stall happens more frequently at lower blade tip speeds. There are hardly any research reports demonstrating the phenomenon; that is why Tirandaz and Rezaeiha [31] set out to investigate the effect of airfoil shape on dynamic stall. Their research on 126 distinct types of airfoils revealed that increasing the leading-edge radius reduces power coefficient in all cases and increased blade thickness can enhance turbine performance at low blade tip speeds, but not at high blade tip speeds [32]. Other studies tried to overcome to problems of H-type rotor Darrius wind turbine with changing in the airfoil shape. Mingwe et al. design a new wind speed self-adapting airfoils, they indicated that in the low TSRs movable flap can improve the wind turbine performance but in the high TSRs has not adventures to wind turbine [33].

The turbine begins to rotate at idle and progresses to the lift regime through passing the drag-lift regime at blade tip speeds less than 1. In drag-lift regime (blade tip speed less than 1), the lift force acts in the opposite direction of the wind, while the drag force acts in the same direction. Fig. 1 (a) depicts the blades' angle of attack at the speed of the blade tip below 1, which reaches 180° in the direction of the wind.

The angle of attack above 90° shows that the drag force acts on the blade. The red path depicts the location of the drag effect. Figs 1 (a) and (b) shows the difference in angle of attack effect for TSRs below and above 1. Researchers have devoted more attention to the operating mechanism of the Darrius turbine with respect to the lift regime due to its higher power coefficient [34–36]. However, the majority of problems with this type of turbine occur in drag-lift regime. The goal of the present study is to use in on the drag-lift regime in order to mitigate the negative impacts of low-starting torque on wind turbines. In this regard, a relation to compute the blade attack angle at blade tip speeds less than 1 is proposed, and the performance of a Darrius type wind turbine with straight blades in the drag-lift regime was explored using numerical analysis. The drag-lift effect of design parameters such as airfoil type, chord length, and airfoil thickness was investigated and then compared to wind turbine performance in the lift domain. Finally, appropriate design parameters were incorporated to ensure effective functioning at low wind speeds and to overcome self-rotation problem. Clearly, the goals of this study are divided into the following three parts: 1) Defining the new equation for calculating the angle of attack in TSRs below one. 2) comparison the performance of Darrius wind turbine in two regimes 3) proposed the appropriate design of Darrius wind turbine to ensure effective functioning at low wind speeds.

1.1. Geometry of simulated wind turbines

Six types of wind turbines with different airfoil shapes and chord lengths were evaluated. Since the goal of this study was to investigate the influence of variations in thickness, chord length, and blade curvature on wind turbine performance at blade tip speeds less than 1, three types of airfoils

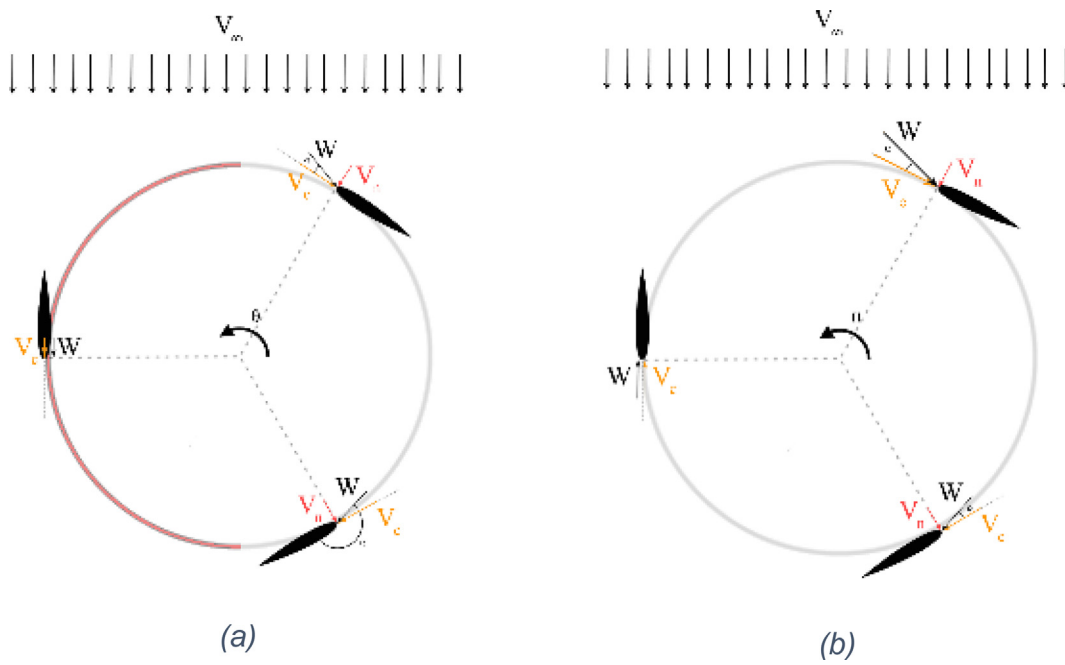


Fig. 1 The velocity components in the rotor area in two situation. a) tip speed ratio below 1b) tip speed ratio above 1.

were chosen with 0.1 and 0.2 m chord length: NACA0018, NACA0022, and NACA4418. The dimension ratio of wind turbines was assumed to be constant and equal to 1. Previous studies have shown that the three-bladed rotor is of advantages such as increased power coefficient at high TSRs and better rotation at low Reynolds [12,20,37,38]. Three wind turbine blades were used for this study. The rotor solidity was computed using Equation (1), and the chord length was the only element influencing the solidity change. The specifications of the simulated turbines are shown in Table 1.

$$\sigma = \frac{Nc}{D} \quad (1)$$

Simulations were performed at 5 different TSRs. Table 2 shows the parameters used in the simulations. The free wind flow velocity was kept at 5 m for simulations, and TSR modifications were performed using the rotor speed. The challenges associated with the self-rotation of Darrius type wind turbines are lessened as the Reynolds number increases, and the primary problems are associated with low Reynolds numbers. Accordingly, the Reynolds number was in the range of $3.5\text{--}7 \times 10^4$. The chord length parameter causes the very change in Reynolds' value. One of the most essential characteristics in

wind turbine operation is the angle of attack. The varied behavior of the angle of attack at TSRs less than and greater than 1 necessitates the use of two separate equations to compute it. Since using the stated relation to determine the angle of attack at TSRs above 1 yields an erroneous result for the angle of attack at TSRs below 1, this study employed the equation (2) to calculate the TSR below 1 and the equation (3) to calculate the TSR above 1.

$$\alpha_u = \tan^{-1} \left(\frac{\sin \theta}{\frac{\lambda}{V/V_\infty} + \cos \theta} \right) \quad (2)$$

$$\alpha_l = \alpha_u + 180 \left(\left[\frac{\alpha_u}{\alpha_u + 1} \right] - \left[\frac{\theta}{180} \right] \right) \quad (3)$$

1.2. Numerical solution

The simulations are based on the solution of incompressible URANS simulations in conjunction with the four equations transition SST turbulence model, all with second-order spatial/temporal discretization. For the pressure-velocity cou-

Table 1 Various simulated wind turbines.

Number	Airfoil	Chord Length (m)	Rotor Height (m)	Rotor Diameter (m)	Rotor Solidity
1	NACA0018	0.1	0.8	0.8	0.375
2	NACA0018	0.2	0.8	0.8	0.75
3	NACA0022	0.1	0.8	0.8	0.375
4	NACA0022	0.2	0.8	0.8	0.75
5	NACA4418	0.1	0.8	0.8	0.375
6	NACA4418	0.2	0.8	0.8	0.75

Table 2 the parameters that used in simulation.

TSR	0.25	0.25	0.25	1.75	2.25
V_∞ (m.s ⁻¹)	5	5	5	5	5
ω (rad.s ⁻¹)	3.125	9.375	15.625	21.875	28.125
Timespan to 1 cycle (s)	2.01	0.67	0.40	0.29	0.223
Time step size	0.558×10^{-5}	0.186×10^{-5}	0.1117×10^{-5}	7.978×10^{-7}	6.205×10^{-7}
Re = [35 × 10 ³ -70 × 10 ³]					

pling, the SIMPLE approach was employed. The commercial CFD package ANSYS Fluent 17.2 was used as the solver. According to previous findings, using the k- ω SST turbulence model can achieve results closer to the experimental data, so in this study, the beforementioned turbulence model was utilized for conducting simulations [25,39]. The simulated geometry was split into stationary and rotary domains. The entire geometry was built with dimensions of 15×25 , and the no-slip requirement was taken into account for the walls. The rectangle's sides were chosen as walls. Turbulent intensity was taken into account at 5 % input, and zero static pressure geometry at the output. Fig. 2 shows the schematic of the computational domain and different regions of the computational grid.

The turbulence model utilized in this study was chosen after a thorough securitized examination of seven commonly used Reynolds averaged eddy-viscosity turbulence models in comparison to three different dissimilar experiments [40] and two more advanced scale-resolving simulations [40,41]. According to the findings, the four-equation transition SST turbulence models are the best-performing eddy-viscosity tools for URANS stimulation of complicated unsteady aerodynamics of VAWTs in dynamic stall. For simulation, the transient mode was used. The time step was taken into account for 0.1° of rotor rotation. A time step of 0.1° was computed based on the rotating speed and time necessary for navigation. The calculated time course for the simulations results in 3600-time steps per turbine cycle. To guarantee that the residues were less than 5–10, 10 rotor rotations were simulated for each simulation, i.e., a total of 36000-time steps. The results presented in this study are for the eleventh rotation of the rotor.

1.3. Validation

Each of the rotors was subjected to four different forms of meshing. The number of nodes divided on the airfoil, the distance of the first layer from the wall, and the degree of rotary domain surface refinement were variables that affected the number of nodes and elements in each mesh, leading to different numerical analysis results for each. The C_p value for the four mesh types developed, which converge in the two final mesh types, shown in Fig. 3. These simulations were performed for TSR 0.75. Finally, type 4 mesh was employed for simulation, and with respect to this, the study's results are reported. The mesh properties are shown in Table 3. The value of y^+ for each mesh indicates that the height of the first layer of mesh from the wall is good.

The numerical grids were validated with laboratory results prior to data curation from the simulation. The turbine recruited for the present study comprises three blades of

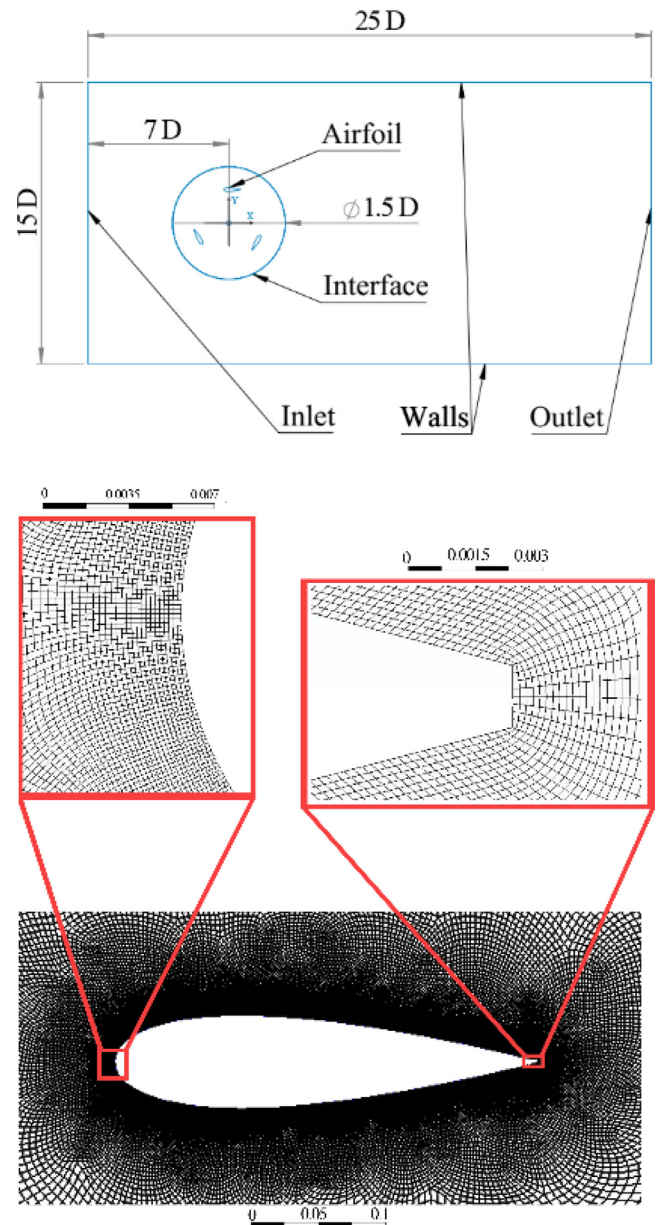


Fig. 2 shows the schematic of the computational domain and different regions of the computational grid.

NACA0015 airfoil, rotor diameter of 1.25 m, and height of 3 m. The wind speed was assumed to be constant at 13.45 m/s. McLaren et al (2012) numerically simulated the

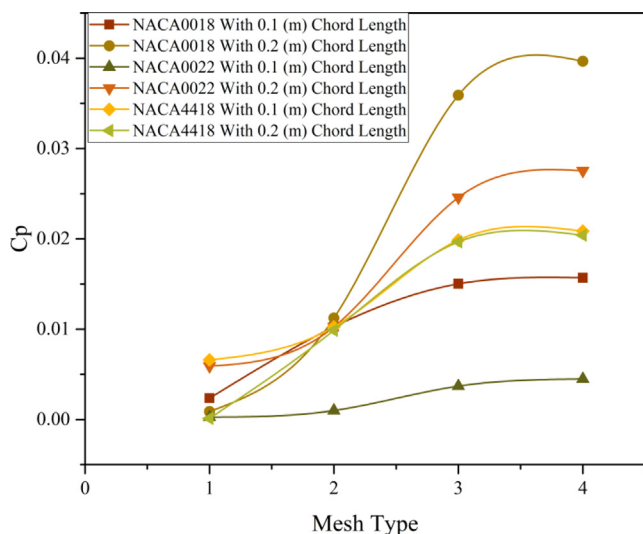


Fig. 3 The power coefficient at TSR 0.75 of 6 simulated turbines in 4 mesh type.

same wind turbine [40]. Two years later, researchers numerically simulated the evaluated turbine again [41]. k- ω SST was used to model the turbulence in both numerical analyses. The simulation findings from the current investigation, as well as the experimental and numerical results from the two previous studies, are displayed in Fig. 4.

Mac and Bass numerical results converge well with the laboratory results from TSR 0.4 to 1.25, however, from TSR 1.25 onwards, the values obtained for C_p revealed greater values for the turbine. The largest discrepancy between the numerical findings of the current study and the laboratory data is noticed at TSR 1.75 and higher, which is related to TSR 2.4, although the general trend of the numerical results of the current study is fairly near to the laboratory results. The overall trend of power coefficient that obtained from numerical simulation of this study with experimental results shows the stability of the results. Finally, to better display the research process a flow-chart of study was drawn. As can see in Fig. 5, qualitative attributes were used for C_p and C_m , which is to compare two wind turbine working regimes.

2. Results and discussion

2.1. The effect of airfoil geometry on power coefficient and torque

The effect of curvature, chord length and airfoil thickness, on power coefficient and torque, was investigated. Turbine perfor-

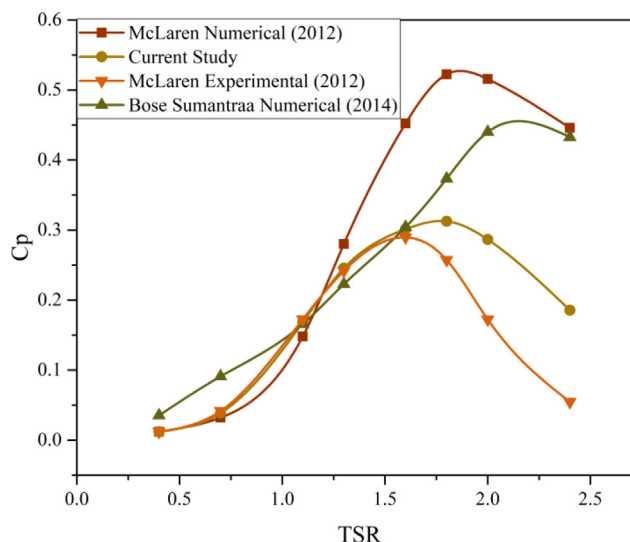


Fig. 4 Comparison of experimental and numerical results of power coefficient of previous studies and current study in 13.45 m/s wind speed.

mance differs at TSR less than 1 and TSR greater than 1. This means that airfoils that provide high turbine performance at TSR below 1 may not be advantageous for the turbine at TSR above 1. Comparing the two airfoils NACA0018 and NACA4418 with a chord length of 0.1 m, the curvature of the airfoil has increased the demand for power and torque (Fig. 6). The researchers discovered that airfoil curvature at lower TSRs would increase turbine performance when compared to NACA0015 and NACA4415 airfoils [42].

However, symmetrical airfoils performed better up to TSR 2.25 with a chord length of 0.2 m. Increasing the chord length definitely improved the wind turbine's performance at TSR less than 1. This is true for all three airfoils. However, at TSR greater than 1, increasing the asymmetric airfoil chord length will cause the turbine to fail. Longer chord length in symmetrical airfoils of NACA0018 and NACA0022 improves C_p at TSR up to 2.25, however, airfoils with shorter chord length performs better at TSR 2.25. Increasing the airfoil thickness from 18 % to 22 % at all tested TSRs reduces turbine performance. This finding is in line with previous studies [43 31].

2.2. Effects of torque and angle of attack on wind turbine performance at different TSRs

Fig. 7 depicts the torque of each turbine blade at TSR 0.25. Fig. (7.a) depicts the output torque of a NACA0018 airfoil tur-

Table 3 mesh properties of six different turbine.

Airfoil	Chord Length (m)	Number of element in rotary domain	Number of element in stationary domain	Grade node on the blade	Maximum y^+
NACA0018	0.1	179,599	22×10^3	250	2.2
NACA0018	0.2	157,659		500	2.1
NACA0022	0.1	168,595		250	2.8
NACA0022	0.2	146,593		500	2.3
NACA4418	0.1	186,592		250	3.5
NACA4418	0.2	175,864		500	3.6

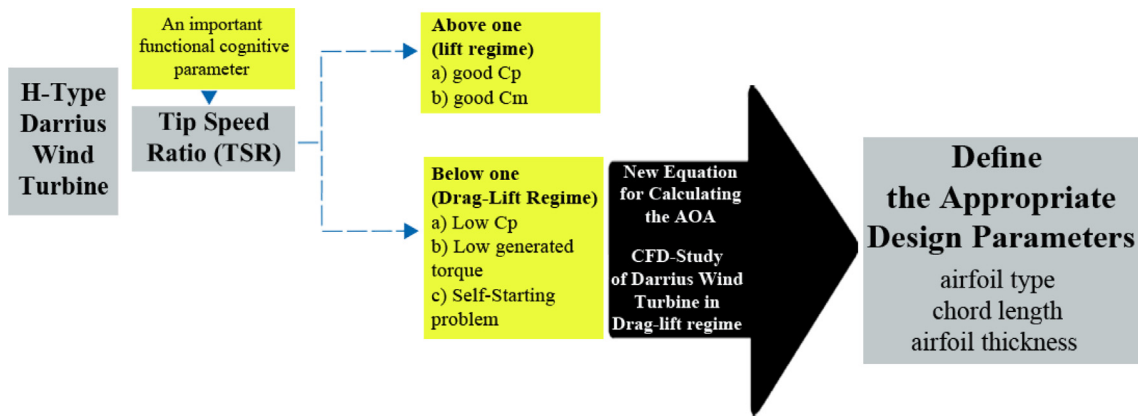


Fig. 5 Flowchart of the research process.

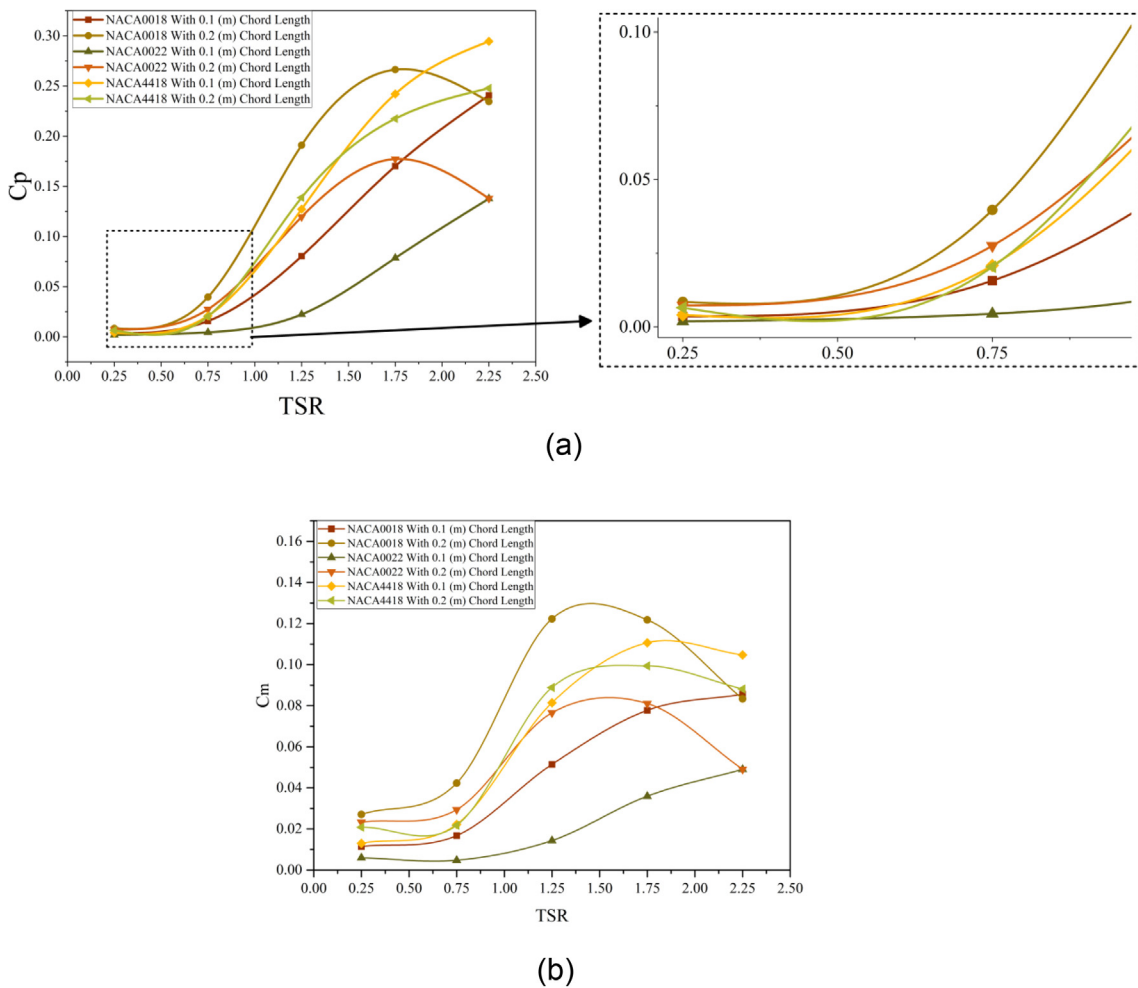


Fig. 6 performance of six different turbines a) power coefficient b) moment coefficient.

bine with a chord length of 0.1 m at 360° from the azimuth angle. The torque produced at angles 15° to 45° and 210° to 240° is considerable for blade number one and is reproduced with a 120° difference for blades two and three. Although there is output torque at other azimuth angles, it is not significant or is negative. Fig. 8 depicts the wind turbine blade attack angle for five different TSRs at azimuth angles ranging from 0° to

360°. The angle of attack at TSR 0.25 and 0.75 was calculated using Equation (3). Fig. 8 shows that after passing an azimuth angle of 100°, the blade will have an angle of attack of more than 90° at TSR 0.25. As a result, if a positive torque is generated at this TSR and the azimuth angle of 100 to 250°, it is due to the drag force of the wind current acting on the blade. By comparing Figs (7.a) and (8), it is clear that the low angle of

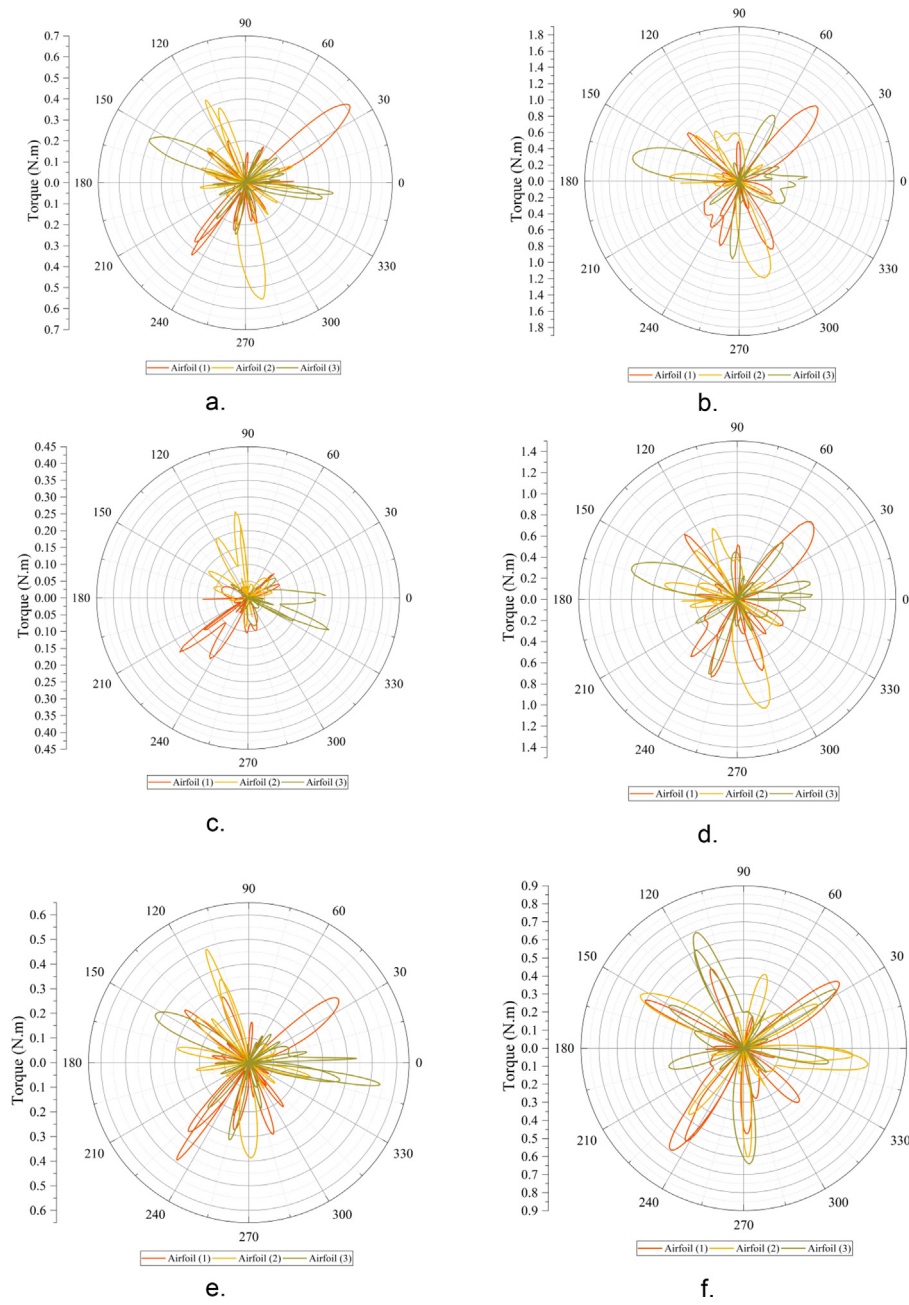


Fig. 7 Generated torque in TSR 0.25 for six turbines.

Label	Blade	Chord length (m)
a	NACA0018	0.1
b	NACA0018	0.2
c	NACA0022	0.1
d	NACA0022	0.2
e	NACA4418	0.1
f	NACA4418	0.2

attack at azimuth angle 15° to 45° , as well as the action of wind flow on the blade as a lift force, have caused torque around the rotor axis, whereas at azimuth angle 210° to 240° , the degree of positive torque produced is due to the drag force. Fig. (7.b) shows the torque produced by the NACA0018 airfoil with a chord length of 0.2. Based on the explanation above, it can be claimed that if a positive torque is generated at an angle of 0° to 90° and 270° to 360° from the azimuth angle, it is due to the lift force, and in the range of 90° to 270° , all positive torques are produced by the drag force. Other researchers have been found that in the critical region, where TSR less than 1, the contribution of the drag to the torque generation plays a significant role in the second and third quarters of the rotor revolution, where the azimuthal position varies between 100° and 253° . [44] Due to the longer airfoil length, the amount of torque caused by drag and lift forces is greater than that of the same blade with a chord length of 0.1 m. It differs for blades with NACA0022 airfoil and chord length 0.1 m. (Fig. (7.c)). Because of the larger blade thickness in this type of turbine, the output torque is exclusively determined by the drag force, and the lift force is unable to rotate the rotor at this TSR. Although the drag interval is greater in this airfoil based on drag force than in the NACA0018 airfoil with 0.1 chord length, the total torque for all three blades is smaller. Increasing airfoil thickness from 18 % to 22 % will exert a significant adverse impact on wind turbine performance. The torque-azimuth angle curve of a turbine with a NACA0022 airfoil with a chord length of 0.2 is shown in Fig. (7.d). Compared to Fig. (7.b), the torque produced in the lift domain is smaller, while the torque produced owing to drag force is greater by 22 %. However, the overall output torque of all three blades for airfoil turbines is higher by 18 %. The curvature of the airfoil increases the positive torque produced by the drag force. The increase in torque owing to drag force is so large that it exceeds the maximum torque generated by the lift force. It is shown in Figs (7.e) and (7.f). The blade number one in Fig. (7.e) has a peak due to the lift force in the azimuth angle range 15° to 45° . Then at angles 105° to 120° , 135° to 150° and 210° to 240° , it has a positive torque due to the drag force. At TSR 0.25, NACA4418 airfoil with a chord length of 0.1 provides greater torque compared to symmetrical airfoils with the same chord length. In the NACA4418 asymmetric turbine with a chord length of 0.2 m, the number of torque peaks generated in consequence of the drag force is greater, however they are not necessarily greater than of the turbine with symmetrical airfoils. This is shown in Fig. (7.f). The torque-azimuth angle curve for six turbines at TSR 2.25 is depicted in Fig. 9. Two TSR 0.25 and 2.25 were employed to further determine the differences in torque generation mechanism at TSRs greater/less than 1. By comparing Fig. 7 with (9), it can be seen that the angle of attack at TSR 2.25 does not exceed 45° . This means that the drag force does not produce positive torque at any azimuth angle. The lift force exists as a factor of positive torque production at all angles. The NACA0018 airfoil with a chord length of 0.1 m is demonstrated in Fig. (9.a). The peak torque produced by blades is 1.6 N.m, each of which generated a positive torque at 120° . The peak torque produced by the NACA0018 airfoil with a length of 0.2 is 3.7, indicating that this airfoil is of high capability to produce torque at TSR 2.25 (Fig. (9.b)). Torque-azimuth angle curve of NACA0022 airfoil with 0.1 m and 0.2 m length is shown in Fig. (9.c) and (9.d). The positive effect

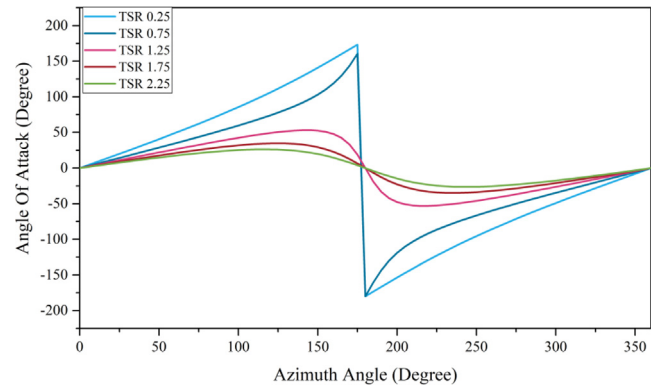


Fig. 8 the wind turbine blade attack angle for five different TSRs.

of increasing the chord length on the output torque can be found upon comparing the two symmetrical airfoils. Previous research has shown that C_p rises with chord length [19]. Since modifying chord length affects rotor solidity, the best range for each turbine must be determined. At TSR 3.06, asymmetric airfoils provided better performance among airfoils with the same chord length, and with increasing curvature for the NACA63A612 airfoils, the maximum C_p occurs at lower TSRs [32]. Fig. (9.e) and (9.f) depicts the output torque for the NACA4418 airfoil. The airfoil's curvature of 44 % has a positive effect on turbine performance, therefore the maximum torque coefficient belongs to this airfoil. The torque peak at TSR 2.25 is larger in the NACA0018 airfoil with a chord length of 0.2 m, however the average positive torque is higher in the NACA4418 airfoil with a chord length of 0.1 m as a consequence of stronger negative torque with respect to this type of airfoil. Comparing Fig. (9.a) and (9.e), it is clear that at TSR 2.25, the curvature of the airfoil minimizes the negative torque produced while increasing the average torque.

Figs. 10 and 11 exhibit graphics from numerical simulations to help understand how the blade attack angle changes. These two schematic graphics are for TSR 0.25 and 2.25. The blades' number one, two, and three are represented in five positions at 23° , 143° , and 263° from the azimuth angle, with a difference of nearly 18° . We can approximate the value of the blade attack angle by tracking the blade after passing the wind flow around it, this is clearly shown in Fig. 10, when TSR is 0.25. The second blade in Fig. 10 is in the drag position and the blade trace is created at the tip of the blade. The position of the blades is the same in both Figs. 10 and 11. The blade trace extends all the way behind the blade, indicating a small attack angle. The lift force is the reason of the positive torque at TSR 2.25 and along the course of the blade, as shown in Fig. 11.

2.3. Torque produced at different TSRs

In order to investigate the influence of airfoils and their behavior at different TSRs, the accumulated torque produced by each of the airfoils is depicted in Figs. 12 to 16.

In each rotation cycle, each of the airfoils produced three notable peaks. The lift force generates peaks at azimuth angles of approximately 45° , 165° , and 285° (Fig. 12). Except for the NACA0022 with a chord length of 0.1 m, all airfoils produced two or three additional peaks due to the drag force between the

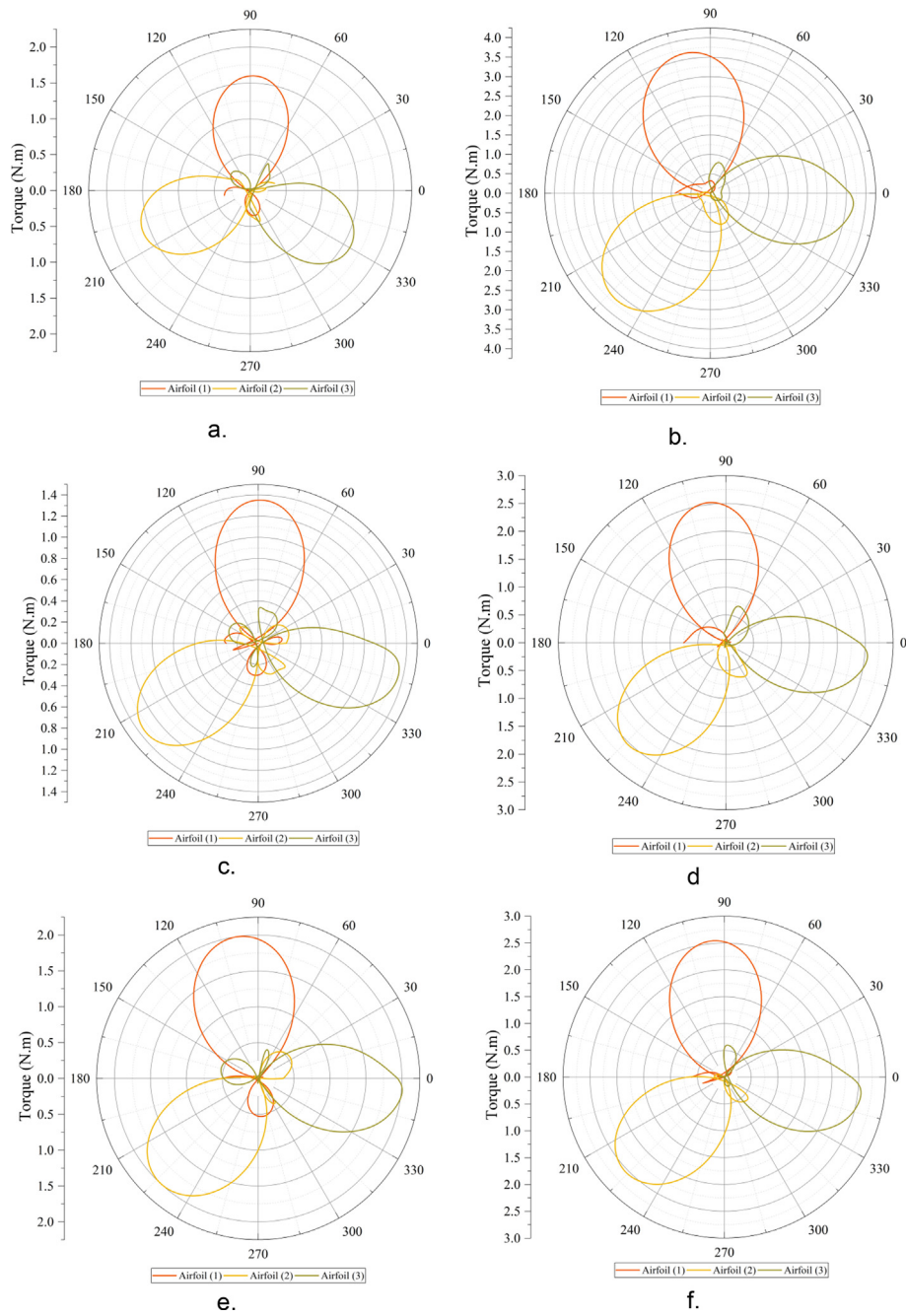


Fig. 9 Generated torque in TSR 1.25 for six turbines.

Label	Blade	Chord length (m)
a	NACA0018	0.1
b	NACA0018	0.2
c	NACA0022	0.1
d	NACA0022	0.2
e	NACA4418	0.1
f	NACA4418	0.2

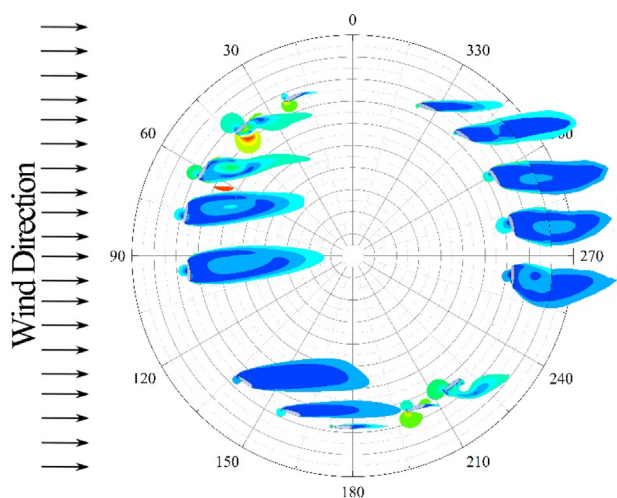


Fig. 10 Contour of speed around blades turbine in TSR 0.25.

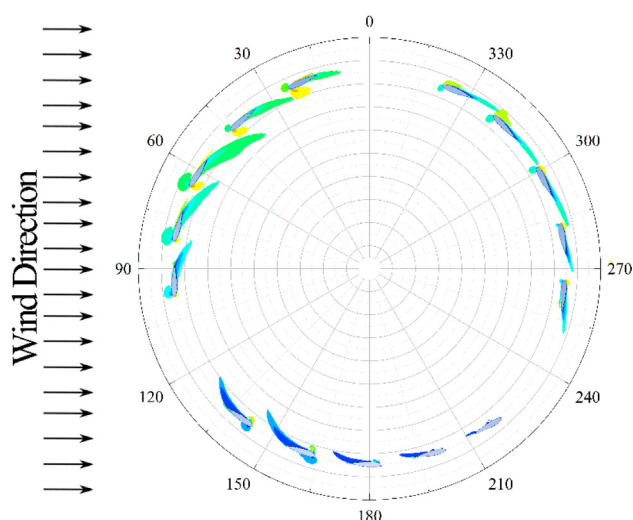


Fig. 11 Contour of speed around blades turbine in TSR 1.25.

two peaks produced by the lift force. The angle of attack, as shown in Fig. 8, is a useful tool for determining the type of torque produced. Due to lift and drag force, all three airfoils with

a chord length of 0.2 m were of higher torque values. Of airfoils with a chord length of 0.1 m, the NACA4418 airfoil produced the maximum torque by virtue of the lift and drag force. Some researches in the literature show that, increasing in thickness of the blade can improve the drag force in low TSRs, this result also achieved in this study [31–32].

At azimuth angles of 115° , 235° , and 355° , it is obvious that the torque due to drag force is greater in asymmetric airfoils (Fig. 12). In Fig. 13, only the torque produced (at TSR 0.75) as the consequence of the lift force had a pick, nevertheless, the torque produced by the drag force is detected for the NACA0022 airfoil with a chord length of 0.1 m at angles 115° , 235° , and 355° from the azimuth angle other airfoils had negative torque in this azimuth angles. At this TSR, the highest positive torque was produced by the NACA0018 airfoil with chord length of 0.2 m. The positive effect of increasing the chord length on the produced torque is evident in two symmetrical airfoils. However, in the case of an asymmetric airfoil, reducing the chord length enhanced wind turbine performance at TSR 0.75. Fig. 14 shows that two symmetrical airfoils with chord length of 0.1 m were of negative torque at TSR 1.25. An asymmetrical airfoil with a chord length of 0.1 m, on the other hand, travels entirely in positive torque. In this TSR (1.25), longer chord length enhances turbine performance in both symmetrical and asymmetrical airfoil regimes, and the optimal turbine performance is associated with the NACA0018 airfoil with 0.2 m chord length. The NACA002 airfoil with 0.1 m chord length had the poorest performance at TSR 1.75 (Fig. 15). The performance of the turbine was enhanced at this TSR by increasing the chord length in symmetrical airfoils, while an asymmetrical airfoil with a shorter chord length gives rise to more uniformity and torque. Fig. 16 shows the torque-azimuth angle curve for TSR 2.25. The performance of the turbine with symmetrical airfoil and longer chord length reduces drastically at this TSR, whereas the airfoil with shorter chord length provides more uniform torque. At this TSR, asymmetric airfoils outperformed symmetrical airfoils, with that the NACA4418 airfoil with 0.1 m chord length having the maximum torque coefficient. Based on the experimental results of the research of Sengupta et al (2016), symmetrical airfoil in the low TSRs can work better than asymmetrical airfoil and in the high wind speed asymmetrical airfoil have better performance [11]. Similarly, this result can be found that in Fig. 16.

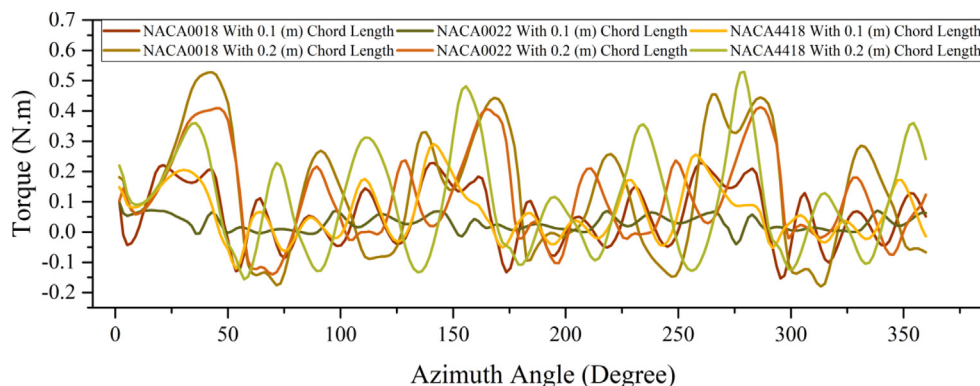


Fig. 12 Generated torque of six wind turbine in TSR 0.25.

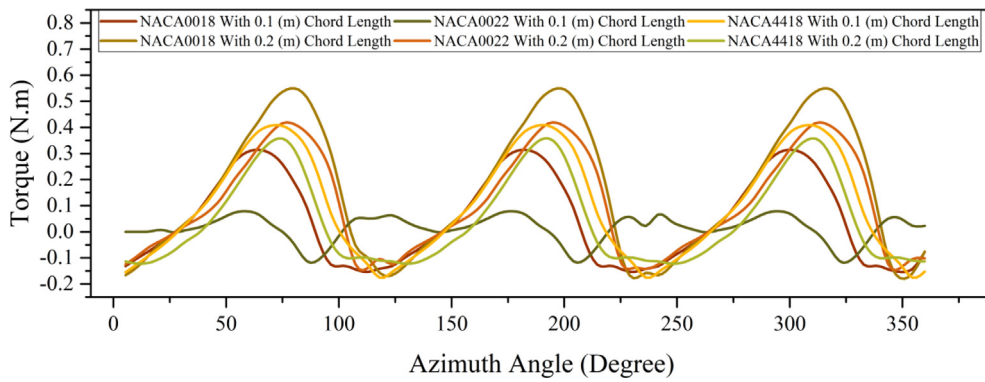


Fig. 13 Generated torque of six wind turbine in TSR 0.75.

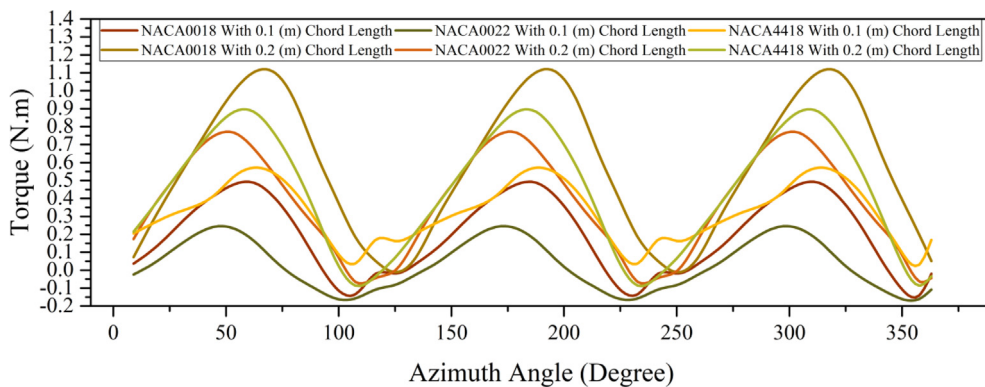


Fig.14 Generated torque of six wind turbine in TSR 1.25.

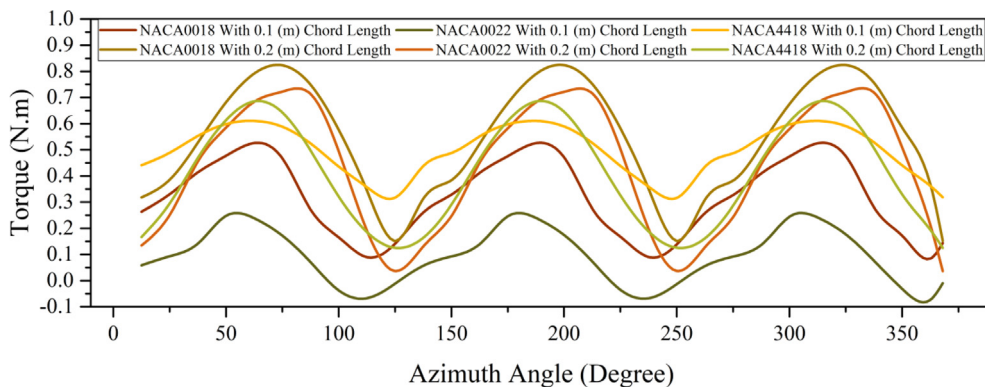


Fig. 15 Generated torque of six wind turbine in TSR 1.75.

3. Conclusions

Rotation in vertical axis wind turbines begins at a standstill mode and progresses to the lift regime after passing through the drag-lift regime. The main problems with this type of turbine are that in drag-lift regime, the initial torque does not overcome the rotational inertia and friction of the mechanical parts of wind turbine, making it difficult or impossible to

achieve TSRs above 1. The purpose of the current study was to determine how to mitigate the aforementioned issues by modifying design parameters such as chord length and airfoil type. In this regard, another goal was to investigate the performance of Darrius vertical axis wind turbines at various TSRs. Computational fluid dynamics method was used to perform the tests. Prior to extracting the results, the independence of the network results was ensured, and the results of the present study were validated with the experimental results and CFD of

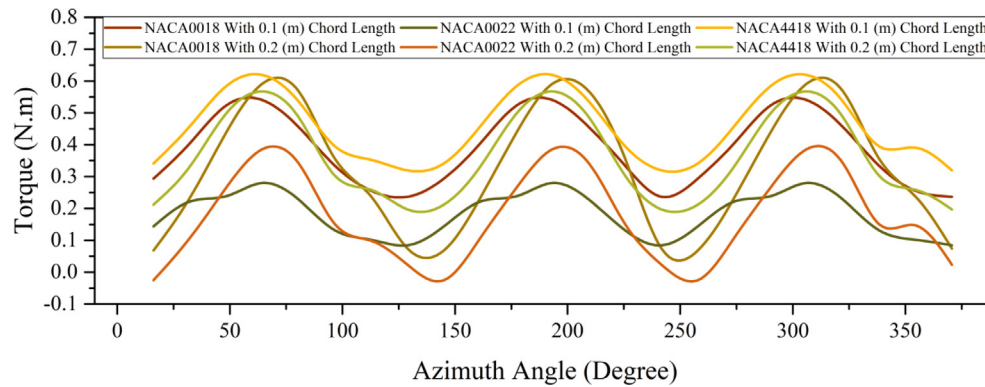


Fig. 16 Generated torque of six wind turbine in TSR 2.25.

the previous studies. The behavior of the turbine differs in drag-lift and lift regimes, so that a change in operation design parameters may improve turbine performance at TSR below one while the same parameters may disrupt turbine performance by increasing TSR over one. The findings from the study can be summarized as follows:

1) Blade thickness

- Increasing the airfoil thickness from 18 % to 22 % reduces turbine performance at all TSRs. However, one of the benefits of increasing the thickness from 18 % to 22 % along the 0.1 m chord is a decrease in negative torque at TSR 0.25.
- One of the problems that airfoils with 22 % of thickness and 0.1 m of chord length have is negative torque in the 0 to 90 degree of azimuth angle at the 0.25 and 0.75 of TSRs. While maximum positive torque appears in this position for other airfoil by lift force.

2) Chord length

- When the TSR is less than 1, increasing the chord length produces more torque due mainly to the lift and drag force. Although the negative points on the torque-azimuth angle curve are deeper for longer chord length airfoils, their average torque is higher.
- At TSR 1.75 onwards, the effect of increasing the chord length will be reversed comparing with the smaller TSRs, causing a decline in turbine performance.

3) Symmetric and asymmetric airfoils

- The curvature of the airfoil particularly exerted effect on the performance of the turbine with chord length of 0.1 m, and this was noticed in both drag-lift and lift regimes. TSR 2.25 provides the maximum C_p for the NACA4418 airfoil.
- Maximum C_p occurs in curved airfoils at upper TSRs. However, at TSRs less than 2, the NACA0018 airfoil with 0.2 m chord length outperformed other airfoils.

4) Overall conclusion

- By comparing the angle of attack obtained from the given relation (3) and the results of the velocity contour around the blade at TSR below 1, one can well understand the behavior of the torque-azimuth angle curve; so that if the angle of attack surpasses 90° , the likelihood of producing positive torque owing to drag force increases. In other

words, positive torque produced at an angle of attack greater than 90° is a direct result of drag-force action on the blade.

Declaration of Competing Interest

The authors declare that they have no known competing financial interests or personal relationships that could have appeared to influence the work reported in this paper.

Acknowledgment

This research was supported by Iran National Science Foundation (INSF) with 98020209 number. We thank our colleagues from INSF who provided insight and expertise that greatly assisted the research.

References

- [1] A. Posa, Influence of Tip speed ratio on wake features of a vertical axis wind turbine, *J. Wind Eng. Ind. Aerodyn.* 197 (2020) 104076.
- [2] M. Elkhoury, T. Kiwata, E. Aoun, Experimental and numerical investigation of a three-dimensional vertical-axis wind turbine with variable-pitch, *J. Wind Eng. Ind. Aerodyn.* 139 (2015) 111–123, <https://doi.org/10.1016/j.jweia.2015.01.004>.
- [3] B. Hand, G. Kelly, A. Cashman, Aerodynamic design and performance parameters of a lift-type vertical axis wind turbine: a comprehensive review, *Renew. Sustain. Energy Rev.* 139 (Apr. 2021), <https://doi.org/10.1016/J.RSER.2020.110699> 110699.
- [4] L. Du, G. Ingram, R.G. Dominy, Experimental study of the effects of turbine solidity, blade profile, pitch angle, surface roughness, and aspect ratio on the H-Darrieus wind turbine self-starting and overall performance, *Energy Sci. Eng.* 7 (6) (2019) 2421–2436, <https://doi.org/10.1002/ese3.430>.
- [5] J.P. Abraham, B.D. Plourde, G.S. Mowry, W.J. Minkowycz, E. M. Sparrow, “Summary of Savonius wind turbine development and future applications for small-scale power generation”, *J. Renew. Sustain Energy* 4 (4) (2012) pp, <https://doi.org/10.1063/1.4747822>.
- [6] M. Johari, M. Jalil, M. S.-I, J. of Engineering, and undefined 2018, “Comparison of horizontal axis wind turbine (HAWT) and vertical axis wind turbine (VAWT),” academia.edu, Accessed: Jan. 23, 2022. [Online]. Available: <https://www>

- academia.edu/download/57615726/IJET_-_Vol._7_4.13_pp_74-80.pdf.
- [7] M. Zemamou, M. Aggour, A. Toumi, Review of savonius wind turbine design and performance, *Energy Procedia*. 141 (2017) 383–388, <https://doi.org/10.1016/j.egypro.2017.11.047>.
- [8] S. ed-Din Fertahi, T. Bouhal, O. Rajad, T. Kousksou, A. Arid, T. El Rhafiki, A. Jamil, A. Benbassou, CFD performance enhancement of a low cut-in speed current vertical tidal turbine through the nested hybridization of savonius and darrius, *Energy Convers. Manage.* 169 (2018) 266–278.
- [9] A. Rezaeiha, I. Kalkman, B. Blocken, CFD simulation of a vertical axis wind turbine operating at a moderate tip speed ratio: guidelines for minimum domain size and azimuthal increment, *Renew. Energy* 107 (Jul. 2017) 373–385, <https://doi.org/10.1016/J.RENENE.2017.02.006>.
- [10] M.A. Singh, A. Biswas, R.D. Misra, Investigation of self-starting and high rotor solidity on the performance of a three S1210 blade H-type Darrius rotor, *Renew. Energy* 76 (Apr. 2015) 381–387, <https://doi.org/10.1016/j.renene.2014.11.027>.
- [11] A.R. Sengupta, A. Biswas, R. Gupta, Studies of some high solidity symmetrical and unsymmetrical blade H-Darrius rotors with respect to starting characteristics, dynamic performances and flow physics in low wind streams, *Renew. Energy* 93 (Aug. 2016) 536–547, <https://doi.org/10.1016/J.RENENE.2016.03.029>.
- [12] P.L. Delafin, T. Nishino, L. Wang, A. Kolios, Effect of the number of blades and solidity on the performance of a vertical axis wind turbine, *J. Phys. Conf. Ser.* 753 (2) (2016) pp, <https://doi.org/10.1088/1742-6596/753/2/022033>.
- [13] H. Beri, Y. Yao, Effect of Camber Airfoil on Self-Starting of VAWT, *J. Environ. Sci. Technol.* (2011) 302–312.
- [14] M.C. Claessens, *The design and testing of airfoils for application in small vertical axis wind turbines*, Delft University of Technology, 2006.
- [15] S. Brusca, R. Lanzafame, M. Messina, Design of a vertical-axis wind turbine: how the aspect ratio affects the turbine's performance, *Int. J. Energy Environ. Eng.* 5 (4) (2014) 333–340, <https://doi.org/10.1007/s40095-014-0129-x>.
- [16] T. Kiwata, T. Yamada, T. Kita, S. Takata, N. Komatsu, S. Kimura, Performance of a vertical axis wind turbine with variable-pitch straight blades utilizing a linkage mechanism, *J. Environ. Eng.* 5 (1) (2010) 213–225, <https://doi.org/10.1299/jee.5.213>.
- [17] A. Sagharichi, M. Zamani, A. Ghasemi, Effect of solidity on the performance of variable-pitch vertical axis wind turbine, *Energy* 161 (Oct. 2018) 753–775, <https://doi.org/10.1016/J.ENERGY.2018.07.160>.
- [18] J.C. Cheng, S.J. Su, J.J. Miao, Application of variable blade pitch control on improving the performance of vertical axis wind turbine, *Appl. Mech. Mater.* 229–231 (2012) 2339–2342, <https://doi.org/10.4028/www.scientific.net/AMM.229-231.2339>.
- [19] T.G. Abu-el-yazied, A.M. Ali, M.S. Al-ajmi, I.M. Hassan, Effect of Number of blades and blade chord length on the performance of darrius wind turbine, *Am. J. Mech. Eng. Autom.* 2 (1) (2015) 16–25.
- [20] Q. Li, T. Maeda, Y. Kamada, J. Murata, K. Furukawa, M. Yamamoto, Effect of number of blades on aerodynamic forces on a straight-bladed Vertical Axis Wind Turbine, *Energy* 90 (Oct. 2015) 784–795, <https://doi.org/10.1016/J.ENERGY.2015.07.115>.
- [21] Y. Wang, X. Sun, X. Dong, B. Zhu, D. Huang, Z. Zheng, Numerical investigation on aerodynamic performance of a novel vertical axis wind turbine with adaptive blades, *Energy Convers. Manag.* 108 (Jan. 2016) 275–286, <https://doi.org/10.1016/J.ENCONMAN.2015.11.003>.
- [22] Q. Li, T. Maeda, Y. Kamada, K. Shimizu, T. Ogasawara, A. Nakai, T. Kasuya, Effect of rotor aspect ratio and solidity on a straight-bladed vertical axis wind turbine in three-dimensional analysis by the panel method, *Energy* 121 (2017) 1–9.
- [23] M. shalby Abdullah Marashli, AlMoThana Gasaymeh, Hani Rawashdeh, “Effect of Specific Geometrical Parameters on the Performance of Small Straight Blade –Vertical Axis Wind turbine (SB-VAWTs) of Darrius-type”, *Int. J. Renew. Energy Res.* (Dec. 2021), <https://doi.org/10.20508/IJRER.V11I4.12420.G8343>.
- [24] E. Mineikis, J. Zakis, and A. Suzdalenko, “Vertical Axis Wind Turbine Performance Based on Rotor Blade Radius,” *IECON Proc. (Industrial Electron. Conf.)*, vol. 2021-October, Oct. 2021, doi: 10.1109/IECON48115.2021.9589582.
- [25] H. Zhu, W. Hao, C. Li, Q. Ding, Numerical study of effect of solidity on vertical axis wind turbine with Gurney flap, *J. Wind Eng. Ind. Aerodynamics* 186 (2019) 17–31.
- [26] C. Liang, D. Xi, S. Zhang, Q. Yang, “Effects of Solidity on Aerodynamic Performance of H-Type Vertical Axis Wind Turbine”, *IOP Conf. Ser. Earth, Environ. Sci.* 170 (4) (Jul. 2018), <https://doi.org/10.1088/1755-1315/170/4/042061>.
- [27] L. Du, G. Ingram, R.G. Dominy, Experimental study of the effects of turbine solidity, blade profile, pitch angle, surface roughness, and aspect ratio on the H-Darrius wind turbine self-starting and overall performance, *Energy Sci. Eng.* 7 (6) (Dec. 2019) 2421–2436, <https://doi.org/10.1002/ESE3.430>.
- [28] X. Sun, J. Zhu, A. Hanif, Z. Li, G. Sun, Effects of blade shape and its corresponding moment of inertia on self-starting and power extraction performance of the novel bowl-shaped floating straight-bladed vertical axis wind turbine, *Sustain. Energy Technol. Assessments* 38 (Apr. 2020), <https://doi.org/10.1016/J.SETA.2020.100648> 100648.
- [29] M. Islam, A. Fartaj, R. Carrière, Design analysis of a smaller-capacity straight-bladed VAWT with an asymmetric airfoil, *Int. J. Sustain. Energy* 30 (3) (2011) 179–192, <https://doi.org/10.1080/1478646X.2010.509496>.
- [30] L.A. Danao, N. Qin, R. Howell, A numerical study of blade thickness and camber effects on vertical axis wind turbines, *Proc. Inst. Mech. Eng. Part A J. Power Energy* 226 (7) (2012) 867–881, <https://doi.org/10.1177/0957650912454403>.
- [31] M.R. Tirandaz, A. Rezaeiha, Effect of airfoil shape on power performance of vertical axis wind turbines in dynamic stall: Symmetric Airfoils, *Renew. Energy* 173 (2021) 422–441, <https://doi.org/10.1016/j.renene.2021.03.142>.
- [32] Y. Wang, S. Shen, G. Li, D. Huang, Z. Zheng, Investigation on aerodynamic performance of vertical axis wind turbine with different series airfoil shapes, *Renew. Energy* 126 (Oct. 2018) 801–818, <https://doi.org/10.1016/J.RENENE.2018.02.095>.
- [33] M. Xu, J. Qu, H. Zhang, Experimental study of vertical axis wind turbine with wind speed self-adapting, *Appl. Mech. Mater.* 215–216 (2012) 1323–1326, <https://doi.org/10.4028/www.scientific.net/AMM.215-216.1323>.
- [34] A. Raj, S. Roy, B. J. Bora, and H. Niyas, “CFD Analysis of a Straight Bladed Darrius Vertical Axis Wind Turbine Using NACA 0021 Aerofoil,” pp. 69–80, 2021, doi: 10.1007/978-981-16-1119-3_6.
- [35] S. Ali and C. M, Jang, “Effects of Tip Speed Ratios on the Blade Forces of a Small H-Darrius Wind Turbine,” *Energies* 2021, Vol. 14, Page 4025, vol. 14, no. 13, p. 4025, Jul. 2021, doi: 10.3390/EN14134025.
- [36] Y. Kumar, A.R. Sengupta, A. Biswas, H.M.S.M. Mazarbhuiya, R. Gupta, CFD Analysis of the Performance of an H-Darrius Wind Turbine Having Cavity Blades, *Lect. Notes Mech. Eng.* (2021) 711–719, https://doi.org/10.1007/978-981-15-7711-6_70.
- [37] Q. Li, T. Maeda, Y. Kamada, J. Murata, K. Furukawa, M. Yamamoto, Effect of number of blades on aerodynamic forces on a straight-bladed vertical axis wind turbine, *Energy* 90 (2015) 784–795, <https://doi.org/10.1016/j.energy.2015.07.115>.
- [38] I. Bel Mabrouk, A. El Hami, Effect of number of blades on the dynamic behavior of a Darrius turbine geared transmission

- system, *Mech. Syst. Signal Process.* 121 (Apr. 2019) 562–578, <https://doi.org/10.1016/J.YMSSP.2018.11.048>.
- [39] J. Chaiyanupong, T. Chitsomboon, Effects of turbulence models and grid densities on computational accuracy of flows over a vertical axis wind turbine, *Int. J. Renew. Energy Dev.* 7 (3) (2018) 213–222, <https://doi.org/10.14710/ijred.7.3.213-222>.
- [40] K. McLaren, S. Tullis, S. Ziada, Computational fluid dynamics simulation of the aerodynamics of a high solidity, small-scale vertical axis wind turbine, *Wind Energy* 15 (3) (Apr. 2012) 349–361, <https://doi.org/10.1002/WE.472>.
- [41] R.B. Sumantraa, S. Chandramouli, T.P. Preamsai, P. Prithviraj, M. Vivek, V.R. Kishore, Numerical analysis of effect of pitch angle on a small scale vertical axis wind turbine, *Int. J. Renew. Energy Res.* 4 (4) (2014) 929–935, <https://doi.org/10.20508/ijrer.50726>.
- [42] M. Islam, D.-K. Ting, A. Fartaj, Desirable Airfoil Features for Smaller-Capacity Straight-Bladed VAWT, *Wind Engineering* 31 (3) (2007) 165–196.
- [43] N.C. Batista, R. Melício, V.M.F. Mendes, M. Calderón, A. Ramiro, On a self-start Darrieus wind turbine: Blade design and field tests, *Renew. Sustain. Energy Rev.* 52 (2015) 508–522, <https://doi.org/10.1016/j.rser.2015.07.147>.
- [44] Y. Celik, L. Ma, D. Ingham, M. Pourkashanian, Aerodynamic investigation of the start-up process of H-type vertical axis wind turbines using CFD, *J. Wind Eng. Ind. Aerodyn.* 204 (Sep. 2020), <https://doi.org/10.1016/J.JWEIA.2020.104252> 104252.